Human Molecular Genetics, 2010, Vol. 19, No. 8 **1603–1617**
doi:10.1093/hmg/ddq036
Advance Access published on January 27, 2010

Genetic studies on the functional relevance of the protein prenyltransferases in skin keratinocytes

Roger Lee[1,†], Sandy Y. Chang[1,†], Hung Trinh[2,4], Yiping Tu[1], Andrew C. White[2,4], Brandon S.J. Davies[1], Martin O. Bergo[5], Loren G. Fong[1], William E. Lowry[2,4,*] and Stephen G. Young[1,3,*]

[1]Department of Medicine, [2]Department of Molecular, Cell and Developmental Biology, [3]Department of Human Genetics and [4]Broad Stem Cell Center, David Geffen School of Medicine, University of California, LA, USA and [5]Wallenberg Laboratory, Institute of Medicine, Sahlgrenska University Hospital, S-413 45 Gothenburg, Sweden

Received December 19, 2009; Revised and Accepted January 25, 2010

The modification of proteins with farnesyl or geranylgeranyl lipids, a process called protein prenylation, facilitates interactions of proteins with membrane surfaces. Protein prenylation is carried out by a pair of cytosolic enzymes, protein farnesyltransferase (FTase) and protein geranylgeranyltransferase type I (GGTase-I). FTase and GGTase-I have attracted interest as therapeutic targets for both cancer and progeria, but very little information exists on the importance of these enzymes for homeostasis of normal tissues. One study actually suggested that FTase is entirely dispensable. To explore the importance of the protein prenyltransferases for normal tissues, we used conditional knockout alleles for *Fntb* and *Pggt1b* (which encode the β-subunits of FTase and GGTase-I, respectively) and a keratin 14–Cre transgene to create mice lacking FTase or GGTase-I in skin keratinocytes. Keratinocyte-specific *Fntb* knockout mice were viable but developed severe alopecia. Although hair follicles appeared normal during development, they were morphologically abnormal after birth, and ultrastructural and immunohistochemical studies revealed many apoptotic cells. The interfollicular epidermis of *Fntb*-deficient mice appeared normal; however, keratinocytes from these mice could not proliferate in culture. As expected, non-farnesylated prelamin A and non-farnesylated DNAJA1 accumulated in *Fntb*-deficient keratinocytes. Keratinocyte-specific *Pggt1b* knockout mice survived development but died shortly after birth. Like *Fntb*-deficient keratinocytes, *Pggt1b*-deficient keratinocytes did not proliferate in culture. Thus, both FTase and GGTase-I are required for the homeostasis of skin keratinocytes.

INTRODUCTION

The post-translational modification of cellular proteins with a 15-carbon farnesyl or a 20-carbon geranylgeranyl lipid (a process generally called protein prenylation) renders proteins more hydrophobic, facilitating interactions with membrane surfaces (1,2). Many but not all prenylated proteins contain a C-terminal *CaaX* motif (*C*, cysteine; *a*, an aliphatic amino acid; *X*, can be one of many residues) (2). The *CaaX* motif triggers the enzymatic addition of a farnesyl or geranylgeranyl lipid to the thiol group of the C-terminal cysteine. When the '*X*' is a leucine or a phenylalanine, the protein is geranylgeranylated by protein geranylgeranyltransferase type I (GGTase-I); otherwise, it is farnesylated by protein farnesyltransferase (FTase) (2). The two protein prenyltransferases share a common α-subunit, but have unique β-subunits that dictate substrate specificities (2). After protein prenylation, the last three amino acids of the protein (i.e. the *aaX*) are released by RAS-converting enzyme 1 (3–5), and the newly exposed isoprenylcysteine is methylated by isoprenylcysteine

*To whom correspondence should be addressed at: Department of Medicine, David Geffen School of Medicine, University of California, 675 Charles Young Dr South, Los Angeles, CA 90095, USA. Tel: +1 3108254934; Fax: +1 3102060865; Email: sgyoung@mednet.ucla.edu (S.G.Y.) or Department of Molecular, Cell and Developmental Biology, David Geffen School of Medicine, University of California, 621 Charles Young Dr South, Los Angeles, CA 90095, USA. Tel: +1 3107945175; Fax: +1 3107949323; Email: blowry@ucla.edu (W.E.L.)
†The authors wish it to be known that, in their opinion, the first two authors should be regarded as joint First Authors.

carboxyl methyltransferase (6,7). Methylation further increases the hydrophobicity of the C-terminus of the protein (7,8).

The protein prenyltransferases have attracted interest because the RAS oncogenes are farnesylated *CaaX* proteins (9,10) and because the cancer-promoting activity of RAS proteins is inhibited when protein prenylation is absent (11). Several pharmaceutical companies have developed inhibitors of the protein prenyltransferases, with most of the effort devoted to inhibitors of protein farnesyltransferases (FTIs) (12–15). FTIs showed promise in preclinical models of cancer (16) and appear to be somewhat efficacious in the treatment of certain leukemias in humans (17). More recently, FTIs have been proposed as a possible therapy for Hutchinson–Gilford progeria syndrome, a disease caused by the accumulation of a farnesylated version of prelamin A (18–20). FTIs improve the hallmark nuclear shape abnormalities in fibroblasts harboring progeria mutations (21,22) and unequivocally ameliorate disease phenotypes in mouse models of progeria (23–26). FTIs are now being tested in children with progeria (19,20,27).

Most of the work on prenyltransferase inhibitors has focussed on blocking the activity of RAS proteins (28–30), and most of the research was performed in the early 1990s before a complete tally of *CaaX* proteins was known. We now know that there are more than 100 protein substrates for FTase and GGTase-I (31,32). Unfortunately, the *in vivo* consequences of inhibiting the prenylation of so many proteins are unknown. One might have imagined that this issue would have already been examined with knockout mouse models, but much of the research on the protein prenyltransferases preceded widespread use of mouse models.

To date, there has been only a single study on the consequences of FTase deficiency in mammals. Several years ago, Mijimolle *et al*. (33) developed a conditional knockout allele for *Fntb*. When their *Fntb* allele was inactivated post-natally by inducing expression of a ubiquitously expressed Cre transgene, few if any pathological consequences were observed, leading the authors to conclude that FTase was dispensable. The apparent dispensability of FTase for adult tissues has raised the possibility that the therapeutic inhibition of FTase might be entirely safe (18). However, the finding that FTase was entirely dispensable in mammals (33) was actually quite surprising, particularly since FTase had been shown to be crucial for the growth and vitality of yeast and plants (34,35). Other findings in Mijimolle's study (33) were also quite unexpected, for example, the observation that HRAS remained associated with cell membranes in the absence of FTase. Other studies have shown that the association of HRAS with membranes is utterly dependent on protein farnesylation (36–39). Recently, Yang *et al*. (40) uncovered a possible explanation for Mijimolle's unexpected findings; they identified an unexpected and previously unrecognized mRNA splicing event in their conditional knockout allele—one that conceivably could yield an enzyme with residual activity. The findings by Yang *et al*. (40) suggested that a re-evaluation of the functional importance of FTase might be needed.

Information is also limited on the *in vivo* importance of GGTase-I in mammalian tissues. Genetic studies by Sjogren *et al*. (41) demonstrated that GGTase-I deficiency interferes with the growth of tumors in mice, but the consequences of GGTase-I deficiency for normal tissues have never been explored.

In the current study, we took advantage of newly developed conditional knockout alleles for *Fntb* (Liu *et al*., submitted for publication) and *Pggt1b* (41) and defined the importance of these enzymes in skin keratinocytes. We chose to examine epidermal keratinocytes because it is possible to obtain high levels of recombination in those cells with the keratin 14–Cre transgene. Furthermore, keratinocytes maintain a delicate balance between proliferation and differentiation, and they produce adnexal structures such as hair—all processes that require complex developmental programs (42). Because prenylated proteins play roles in cell growth, cell–cell interactions and regulation of cell shape (1,2), we suspected that one or both of the protein prenyltransferases might be crucial for homeostasis of skin. Indeed, our genetic studies in mice demonstrated that both enzymes are vital for skin keratinocytes.

RESULTS

We used an *Fntb* conditional knockout allele, $Fntb^{fl}$ (M. Liu *et al*., submitted for publication; Fig. 1A and B), and a keratin 14–Cre (*KCre*) transgene to produce mice lacking FTase in stratified epithelial cells. Keratinocyte-specific *Fntb* knockout mice ($Fntb^{fl/fl}KCre^{+}$, designated $Fntb^{\Delta/\Delta}$) were born at the expected Mendelian frequency. Skin keratinocytes from newborn $Fntb^{\Delta/\Delta}$ mice contained only trace levels of *Fntb* transcripts, as judged by quantitative polymerase chain reaction (PCR) ($2.5 \pm 0.3\%$ of levels in wild-type keratinocytes; $n = 2$ wild-type and $n = 5$ $Fntb^{\Delta/\Delta}$ keratinocyte preparations). Consistent with those results, the β-subunit of FTase (FNTB) was undetectable in keratinocyte extracts, as judged by western blots with an FNTB-specific antibody (Fig. 1C).

The absence of FTase was accompanied by reduced farnesylation of keratinocyte proteins. Western blots of $Fntb^{\Delta/\Delta}$ keratinocyte extracts with a DNAJA1-specific antibody revealed that the majority of the DNAJA1 was non-farnesylated (Fig. 1D and E). Also, $Fntb^{\Delta/\Delta}$ keratinocytes exhibited a striking accumulation of prelamin A. A prelamin A band was obvious on western blots with antibodies against prelamin A or mature lamin A (top and middle panels, respectively, of Fig. 1F). In western blots with the lamin A antibody, the mature lamin A band was detectable, but was less intense than the prelamin A band. The prelamin A in $Fntb^{\Delta/\Delta}$ keratinocytes did not appear to be farnesylated, as judged by its retarded electrophoretic mobility (Fig. 1G). The prelamin A in $Fntb^{\Delta/\Delta}$ keratinocytes co-migrated with the non-farnesylated prelamin A in FTI-treated wild-type cells, and the prelamin A in $Fntb^{\Delta/\Delta}$ keratinocytes migrated slightly more slowly than the farnesyl-prelamin A in $Zmpste24^{-/-}$ keratinocytes (ZMPSTE24 is the enzyme required for the conversion of farnesyl-prelamin A to mature lamin A) (Fig. 1G). As expected, HRAS was found in the S100 (cytosolic) fraction in $Fntb^{\Delta/\Delta}$ keratinocytes, but was located in the P100 (membrane) fraction of wild-type cells (Fig. 1H).

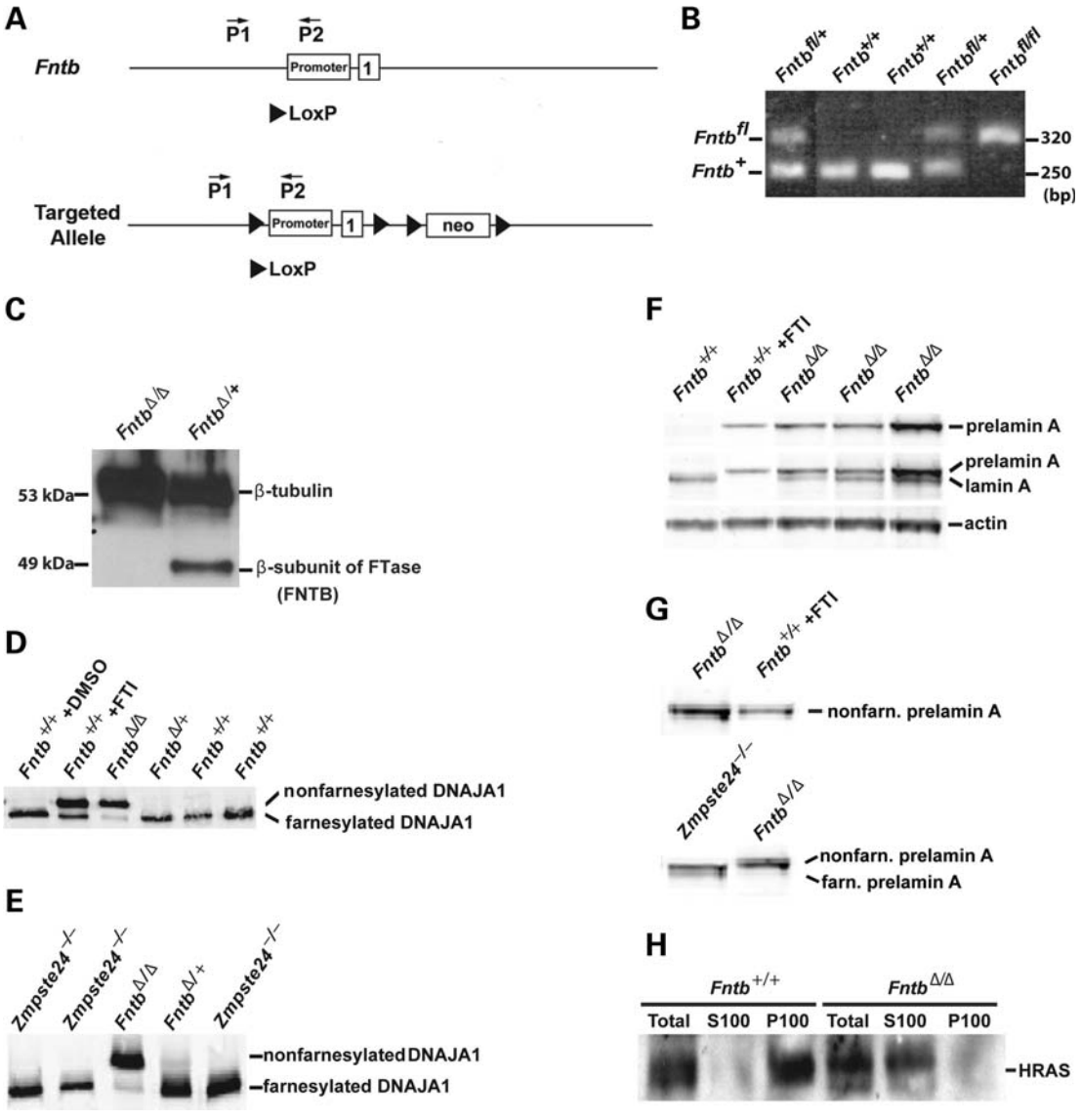

Figure 1. Inactivating FTase in keratinocytes. (**A**) Wild-type and conditional knockout alleles for *Fntb* ($Fntb^{+}$ and $Fntb^{fl}$, respectively). *LoxP* sites, indicated by a triangle, are located upstream of the *Fntb* promoter and in intron 1. (**B**) PCR-amplified fragments of $Fntb^{+}$ and $Fntb^{fl}$ alleles, generated with the indicated primers, could be resolved on an ethidium bromide-stained 1.5% agarose gel. (**C**) Western blot of wild-type and $Fntb^{\Delta/\Delta}$ keratinocytes with an antibody against the β-subunit of FTase (FNTB); β-tubulin was used as a loading control. (**D**, **E**) Western blot of keratinocyte extracts with a DNAJA1-specific monoclonal antibody, revealing that most of the DNAJA1 in $Fntb^{\Delta/\Delta}$ keratinocytes was non-farnesylated. As a control, we examined DNAJA1 in cells that had been treated with an FTI (ABT-100, 5 μM). (**F**) Western blot of keratinocyte extracts with antibodies against prelamin A (top panel) or mature lamin A (the mature lamin A antibody binds both prelamin A and mature lamin A) (middle panel). Actin was used as a loading control. (**G**) Western blot with a prelamin A-specific polyclonal antibody showing that the prelamin A in $Fntb^{\Delta/\Delta}$ keratinocytes co-migrates with non-farnesylated prelamin A in FTI-treated cells and migrates slightly more slowly than farnesylated prelamin A in $Zmpste24^{-/-}$ fibroblasts (56). (**H**) Western blots of HRAS in total cell extracts and P100 and S100 fractions of wild-type and $Fntb^{\Delta/\Delta}$ keratinocytes.

We suspected that we might be able to observe an accumulation of prelamin A in the skin of $Fntb^{\Delta/\Delta}$ mice by immunohistochemistry. In early immunohistochemistry experiments with a prelamin A antibody developed by Fong *et al*. (43) and several commercial antibodies, we were disappointed by a high level of background staining. For that reason, rats were immunized with a peptide corresponding to the last 18 amino acids of mouse prelamin A. A rat with a strong immune response was used to develop a prelamin A-specific monoclonal antibody (antibody 7G11). Antibody 7G11 bound avidly to the non-farnesylated prelamin A in FTI-treated fibroblasts, but did not bind to lamin A or lamin C (Fig. 2A and B). In immunohistochemistry studies, prelamin A staining with antibody 7G11 was undetectable in wild-type skin keratinocytes (Fig. 2C), but was intense in keratinocytes from $Fntb^{\Delta/\Delta}$ mice (Fig. 2D). As expected, prelamin A in $Fntb^{\Delta/\Delta}$ skin was confined to keratinocytes expressing K14 and was undetectable in the dermal fibroblasts (Fig. 2D). Prelamin A was undetectable in the skin keratinocytes of mice lacking GGTase-I ($Pggt1b^{\Delta/\Delta}$) (Fig. 2E), but was found in the skin keratinocytes of mice lacking both FTase and GGTase-I ($Fntb^{\Delta/\Delta}Pggt1b^{\Delta/\Delta}$) (Fig. 2F). As expected,

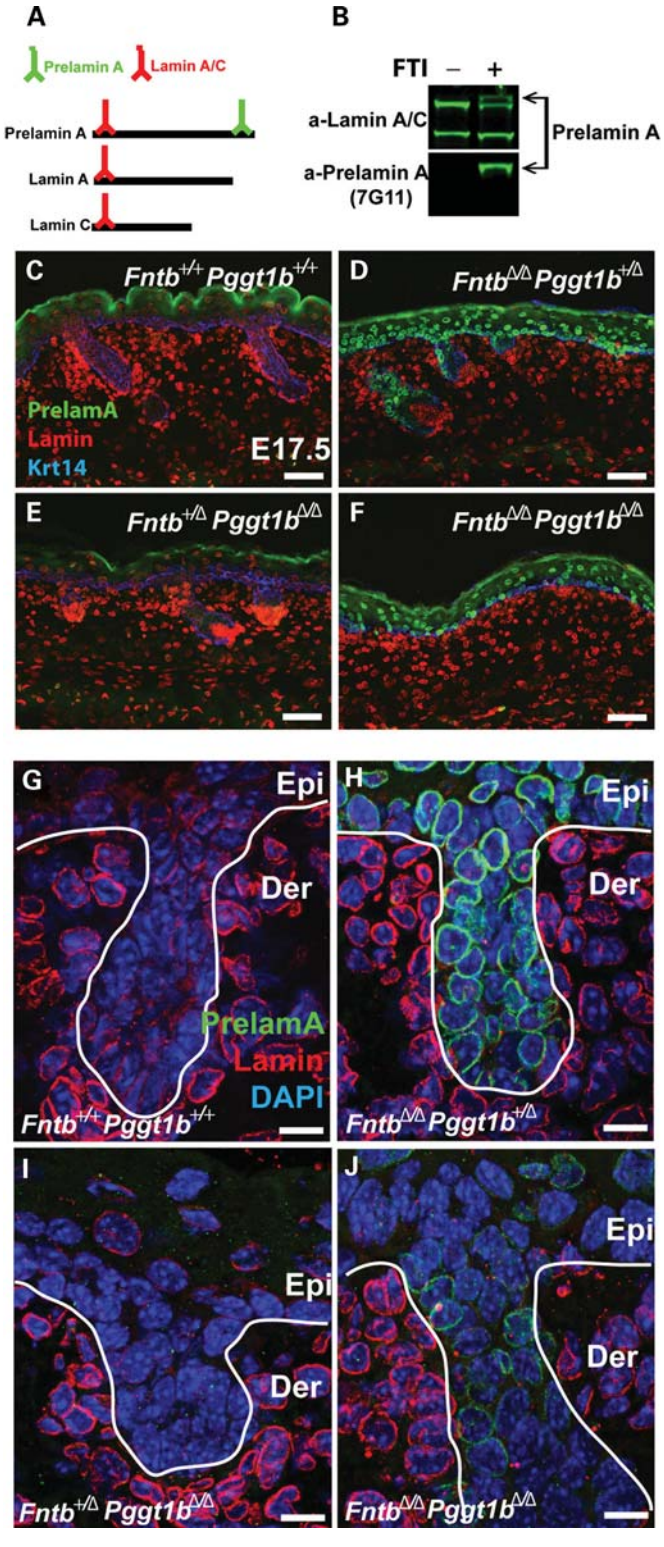

Figure 2. Experiments with a new rat monoclonal antibody against prelamin A, 7G11, showing that prelamin A accumulates in *Fntb*$^{\Delta/\Delta}$ keratinocytes. (**A**) Schematic depicting prelamin A, lamin A and lamin C and their recognition by the indicated antibodies. (**B**) Western blot of wild-type fibroblasts in the presence and absence of an FTI (ABT-100, 5 μM), showing that antibody 7G11 binds avidly to non-farnesylated prelamin A (lower panel). The detection of lamin A, lamin C and prelamin A with an N-terminal lamin A/C antibody is shown in the upper panel. (**C**–**J**) Immunohistochemical staining of skin with the prelamin A-specific antibody 7G11, a polyclonal antibody against lamins A/C and an antibody against keratin 14 at embryonic day 17.5. (C, G) Skin from a wild-type mouse (*Fntb*$^{+/+}$*Pggt1b*$^{+/+}$). (D, H) Skin from an *Fntb*$^{\Delta/\Delta}$*Pggt1b*$^{+/\Delta}$ mouse. (E, I) Skin from an *Fntb*$^{+/\Delta}$*Pggt1b*$^{\Delta/\Delta}$ mouse. (F, J) Skin from an *Fntb*$^{\Delta/\Delta}$*Pggt1b*$^{\Delta/\Delta}$ mouse. Scale bars for (C–F) are 50 μm and for (G–J) 16 μm.

prelamin A accumulated in both keratinocytes and dermal fibroblasts of *Zmpste24*$^{-/-}$ mice, but was confined to keratinocytes in *Fntb*$^{\Delta/\Delta}$ mice (Supplementary Material, Fig. S1). Interestingly, higher power images revealed that most of the prelamin A in *Fntb*$^{\Delta/\Delta}$ and *Fntb*$^{\Delta/\Delta}$*Pggt1b*$^{\Delta/\Delta}$ keratinocytes was located at the nuclear rim (Fig. 2G–J).

Fntb$^{\Delta/\Delta}$mice could be distinguished from littermates on post-natal day 6 (P6) by alopecia (hair normally becomes visible at P6 when the hair shafts emerge from follicles) (Fig. 3A). The alopecia was virtually complete and persisted throughout life (Fig. 3A). *Fntb*$^{\Delta/\Delta}$mice were smaller than unaffected littermates, but appeared to be healthy and survived normally (some *Fntb*$^{\Delta/\Delta}$mice were maintained in the colony for $>$300 days).

Hematoxylin and eosin-stained sections of *Fntb*$^{\Delta/\Delta}$skin revealed that the hair follicles in post-natal *Fntb*$^{\Delta/\Delta}$mice were stunted in appearance (both shorter and narrower) (Fig. 3B). Some follicles from *Fntb*$^{\Delta/\Delta}$mice contained hair shafts, but most of the hair shafts were dysmorphic and improperly angled and few penetrated the surface of the skin (Fig. 3B). The hair follicles appeared normal at embryonic day 17.5 (E17.5), but stunting of hair follicles was easily apparent at all post-natal time points (Fig. 4A).

Hair follicle stem cells express Sox9 and can first be detected during epidermal development by immunohistochemistry with Sox9-specific antibodies (44). Interestingly, Sox9 staining was normal in *Fntb*$^{\Delta/\Delta}$ mice, suggesting that *Fntb* deficiency has little effect on the formation of the stem cell compartment (Fig. 4B). The matrix, located at the base of the hair follicle, contains proliferating cells that differentiate to form hair shafts. Immunohistochemical staining for the matrix marker CDP (CCAAT displacement protein) was normal in *Fntb*$^{\Delta/\Delta}$mice, although the size of the matrix was smaller than that in wild-type mice (Fig. 4C). Staining for keratin 31, a marker of the hair cortex, was detectable in *Fntb*$^{\Delta/\Delta}$ mice, but the staining was less intense (Fig. 4D). Electron microscopy of skin from *Fntb*$^{\Delta/\Delta}$mice revealed that all of the appropriate layers of the hair shaft were generated but the hair shafts were smaller and not as straight as those of wild-type mice (Fig. 5A).

There were no obvious morphological defects in the interfollicular epidermis in *Fntb*$^{\Delta/\Delta}$mice, as judged by routine histology (Figs 3B and 4A), and staining for markers of epidermal differentiation did not uncover any abnormalities (Supplementary Material, Fig. S2). Also, electron microscopy showed that all layers of the epidermis were intact (Fig. 5B). The absence of pathology in the interfollicular epidermis, either by light or electron microscopy, led us to predict that skin barrier function in *Fntb*$^{\Delta/\Delta}$mice would be normal. Indeed, barrier function assays in E19.5 *Fntb*$^{\Delta/\Delta}$mice uncovered no abnormalities (Supplementary Material, Fig. S3A).

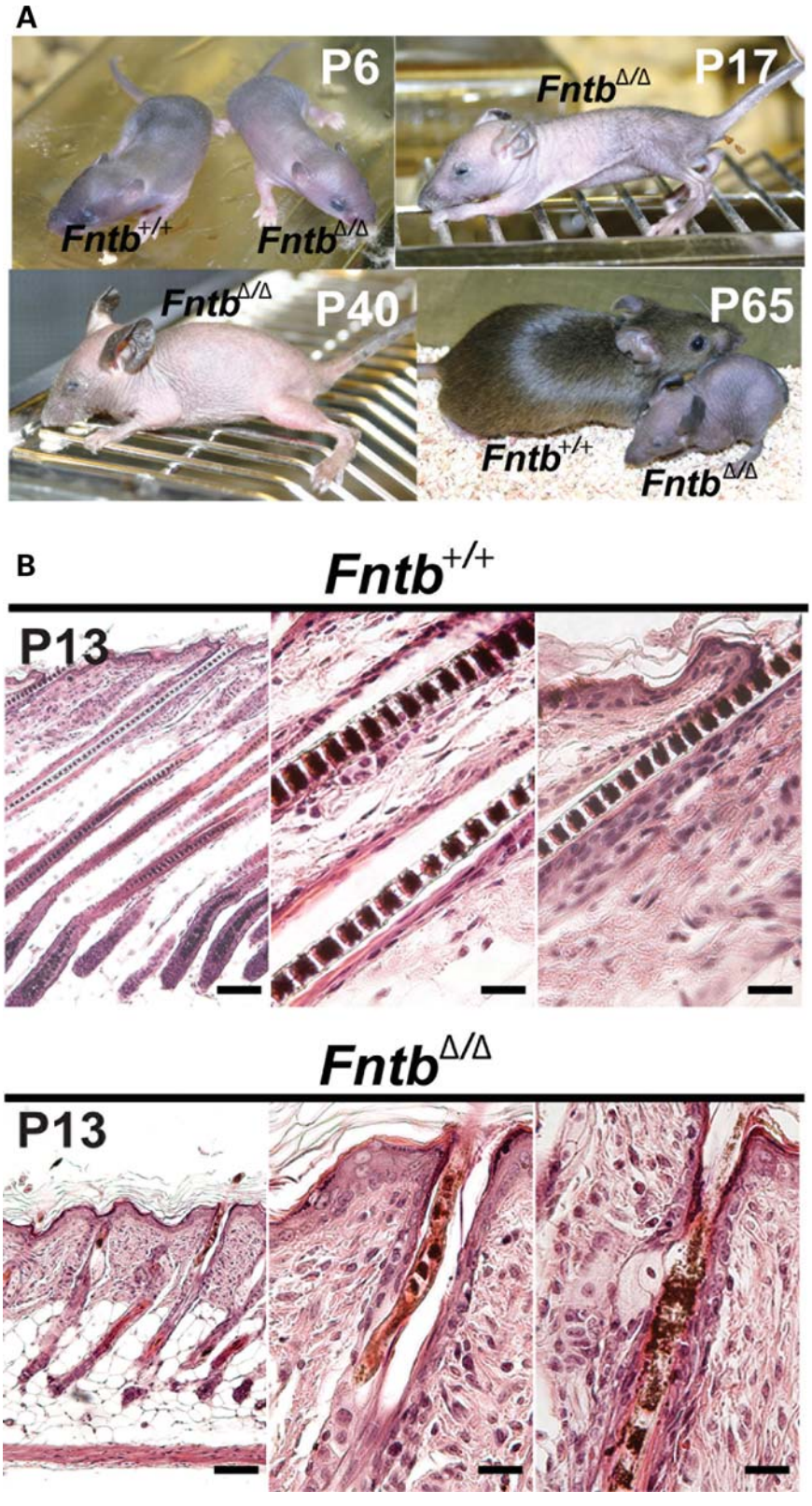

Figure 3. Alopecia in keratinocyte-specific *Fntb* knockout mice (*Fntb*$^{\Delta/\Delta}$). (**A**) Alopecia in *Fntb*$^{\Delta/\Delta}$ mice was detectable by close visual inspection on post-natal day 6 (P6) but was obvious at later time points (P17, P40, P65). (**B**) Hematoxylin and eosin-stained sections of skin from *Fntb*$^{+/+}$ and *Fntb*$^{\Delta/\Delta}$ mice at P13. Hair follicles in *Fntb*$^{\Delta/\Delta}$ mice were stunted compared with those of *Fntb*$^{+/+}$ mice, and the morphology of hair shafts was abnormal. Scale bars indicate 100 μm for left panels and 25 μm for middle and right panels.

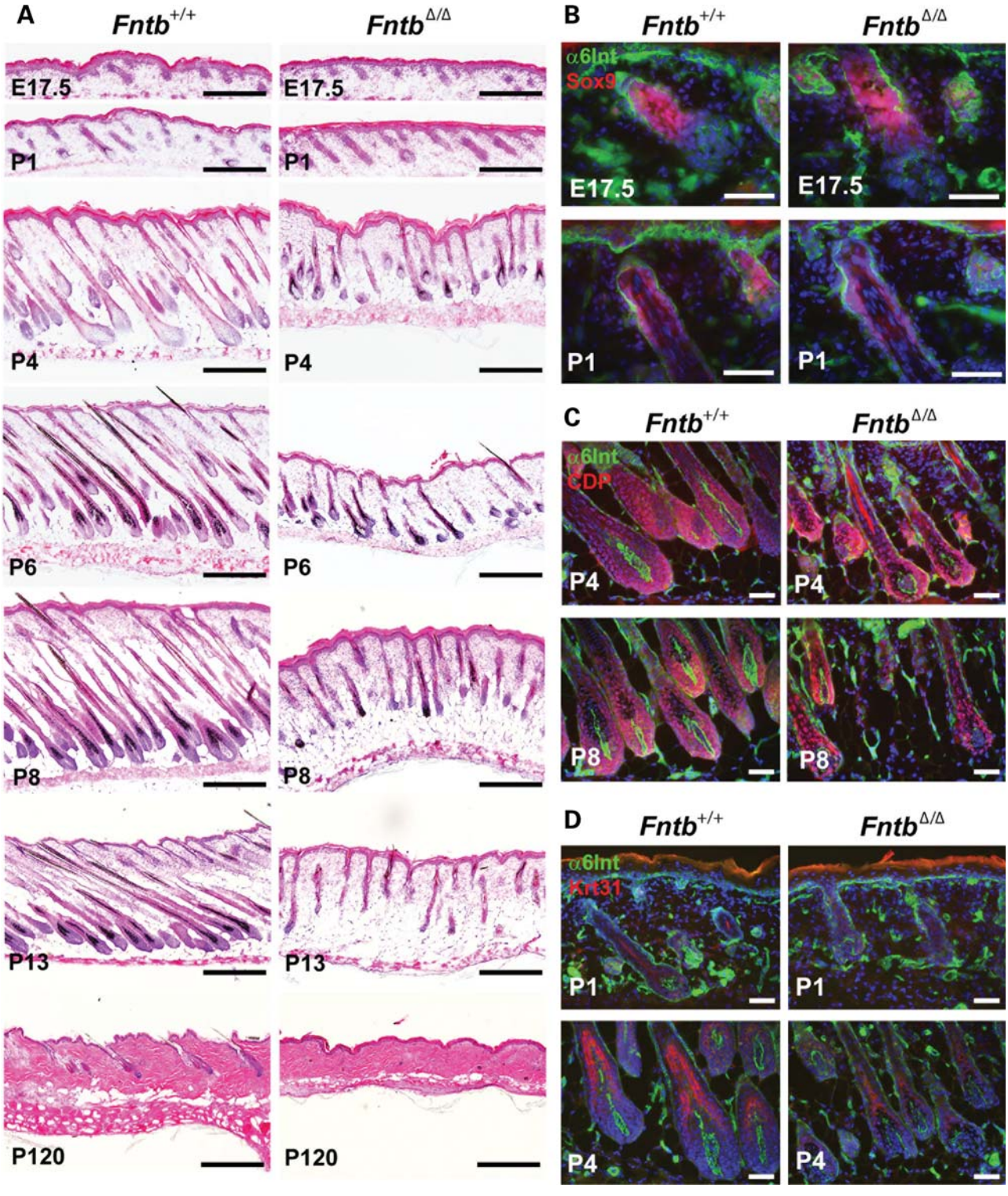

Figure 4. Analysis of alopecia in keratinocyte-specific *Fntb* knockout mice ($Fntb^{\Delta/\Delta}$). (**A**) Hematoxylin and eosin-stained sections of skin from $Fntb^{+/+}$ and $Fntb^{\Delta/\Delta}$ mice at different time points. At P120, few hair follicles remained in $Fntb^{\Delta/\Delta}$ mice. (**B**) Immunohistochemical staining of skin from $Fntb^{+/+}$ and $Fntb^{\Delta/\Delta}$ mice with an antibody against the stem cell marker Sox9 (red) indicates that the stem cell compartment is relatively unaffected by FTase deficiency. An antibody against α6-integrin (α6-Int, green) was used to demark epidermal structures. (**C**) Immunohistochemical staining of skin from $Fntb^{+/+}$ and $Fntb^{\Delta/\Delta}$ mice with an antibody against CDP (red), a marker of the follicular transit-amplifying population shows that the matrix of the hair follicle is present, even in the absence of FTase. However, the hair matrix was smaller in $Fntb^{\Delta/\Delta}$ mice. (**D**) Immunohistochemical staining of skin from $Fntb^{+/+}$ and $Fntb^{\Delta/\Delta}$ mice with an antibody against keratin 31 (red), which is expressed in differentiating cells of the hair follicle. Keratin 31 was present in $Fntb^{\Delta/\Delta}$ hair follicles, but fewer positive cells were detected. Scale bars indicate 50 μm for (B–D) and 200 μm for (A).

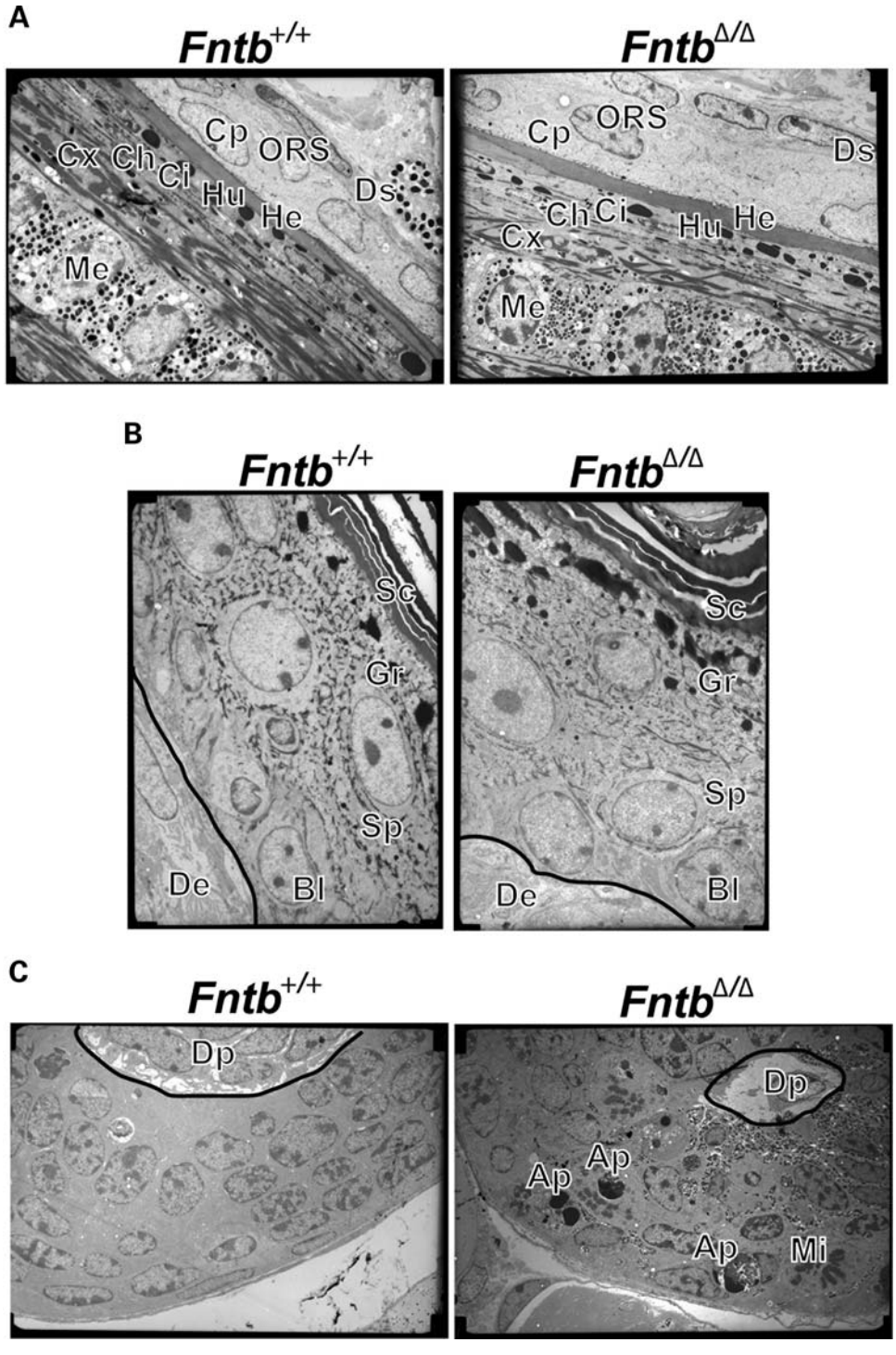

Figure 5. Electron microscopy of skin in *Fntb*$^{+/+}$ and *Fntb*$^{\Delta/\Delta}$ mice. (**A**) Electron micrographs of hair shafts, revealing that all layers of the hair shaft are present in *Fntb*$^{\Delta/\Delta}$ mice, but the hair shafts were smaller than those in *Fntb*$^{+/+}$ mice. Each layer of the follicle is demarcated: Ds, dermal sheath; ORS, outer root sheath; Cp, companion layer; He, Henley's layer; Hu, Huxley's layer; Ch and Ci, cuticle layers; Cx, cortex; Me, medulla. (**B**) Electron micrographs, showing that all layers of the interfollicular epidermis are intact in *Fntb*$^{\Delta/\Delta}$ mice. De, dermis; Bl, basal layer; Sp, spinous layer; Gr, granular layer; Sc, stratum corneum. (**C**) Electron micrographs of the hair follicle matrix in *Fntb*$^{+/+}$ and *Fntb*$^{\Delta/\Delta}$ mice, revealing multiple apoptotic epithelial cells (Ap) and mitotic cells (Mi) in the matrix of the hair follicle (Mi) in *Fntb*$^{\Delta/\Delta}$ mice. Images were acquired at 2900×.

We examined immunohistochemical markers for cell division and apoptosis in the skin of *Fntb*$^{\Delta/\Delta}$ and control mice. Staining for the phosphorylated form of histone H3 (phosphoH3), a marker of cell mitosis, appeared to be normal in *Fntb*$^{\Delta/\Delta}$ mice (Fig. 6A). Staining for another marker of dividing cells, Ki67, was also normal in *Fntb*$^{\Delta/\Delta}$ skin (Fig. 6B). To identify apoptotic cells, skin was stained with an antibody recognizing the cleaved form of caspase 3. Apoptotic cells

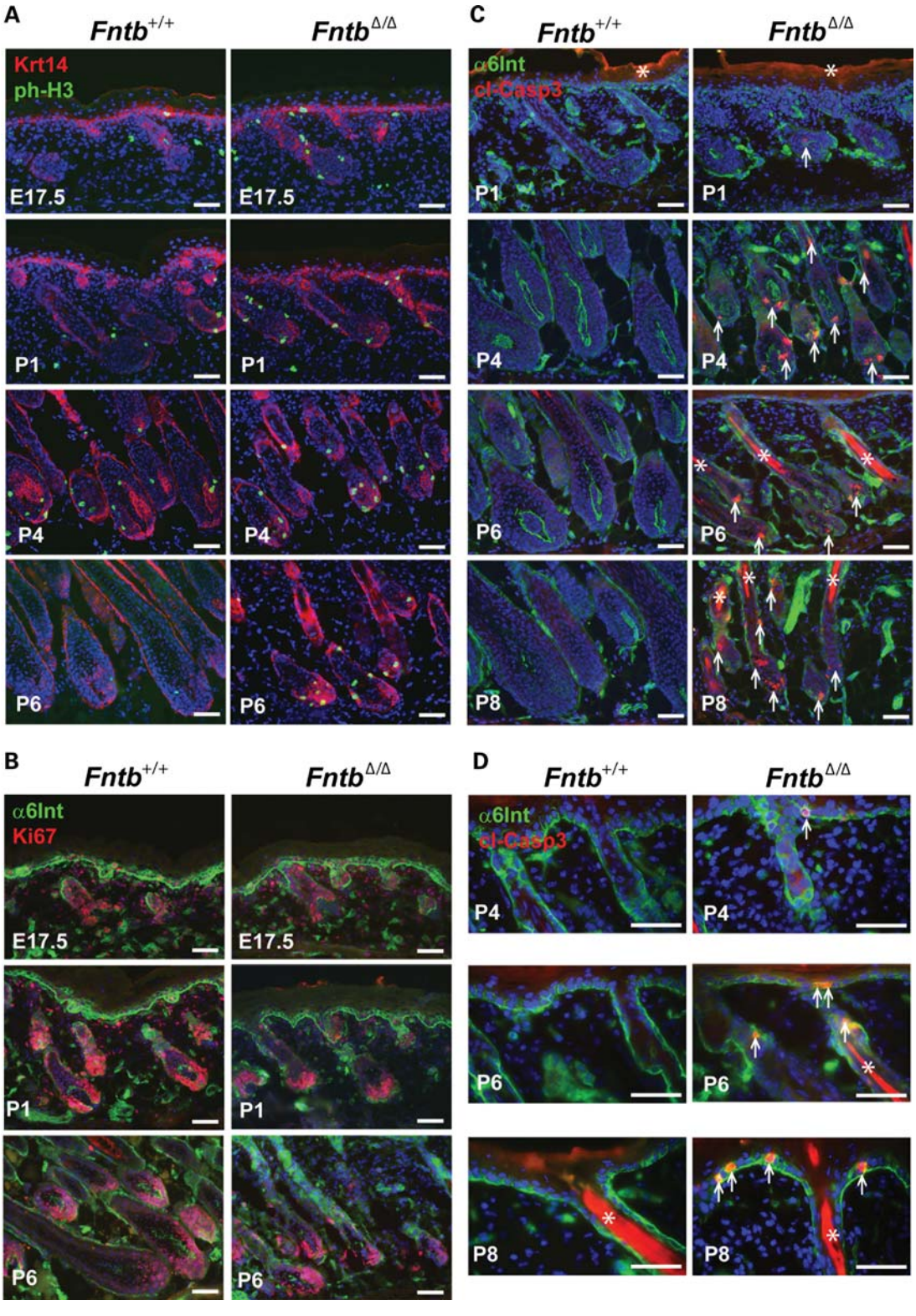

Figure 6. *Fntb* deficiency in the epidermis does not affect proliferation in hair follicles but leads to increased numbers of apoptotic cells. (**A**) Immunohistochemical staining of skin with an antibody against phosphorylated histone-H3 (ph-H3, green), a marker of cell proliferation, reveals similar levels of staining in $Fntb^{+/+}$ and $Fntb^{\Delta/\Delta}$ mice. Keratin 14 staining (red) was used to demark epidermal cells. (**B**) Immunohistochemical studies with another marker of cell proliferation, Ki67, revealing many dividing cells in the skin from both $Fntb^{+/+}$ and $Fntb^{\Delta/\Delta}$ mice. (**C**) Immunohistochemical studies with an antibody against the cleaved form of caspase 3 (cl-Casp3, red), a marker of apoptotic cells, uncovered apoptotic cells in the hair follicles of $Fntb^{\Delta/\Delta}$ mice (arrows) but not in $Fntb^{+/+}$ mice. Hair shafts have a high level of autofluorescence (asterisks). (**D**) Additional immunohistochemical studies, focussing on the interfollicular epidermis, with an antibody against the cleaved form of caspase 3 (red). Apoptotic cells (arrows) could be identified in the interfollicular epidermis of $Fntb^{\Delta/\Delta}$ mice. Scale bars indicate 50 μm for (A–D).

are normally found in hair follicles only during the catagen phase of the hair cycle, which begins around P15, but apoptosis is normally absent in P1–P8 skin. In $Fntb^{\Delta/\Delta}$ mice, apoptotic cells were detected in the hair follicle at P1 and were even more numerous at P4, P6 and P8 (Fig. 6C), providing a plausible explanation for the stunted morphology of the hair follicles. To explore this issue further, we examined the hair follicles of $Fntb^{\Delta/\Delta}$ and control mice by electron microscopy. Numerous apoptotic cells were identified in the hair follicle matrix of $Fntb^{\Delta/\Delta}$ mice at P6, whereas none was found in control mice (Fig. 5C).

Scattered apoptotic cells were also found in the interfollicular epidermis of $Fntb^{\Delta/\Delta}$ mice at P4, P6 and P8 (Fig. 6D). Why apoptosis was associated with clear-cut pathology in hair but less so in interfollicular epidermis is unknown, but one possibility is that dying cells are replaced more effectively in the interfollicular epidermis. Consistent with this notion, hair follicles had largely disappeared by P120, whereas the interfollicular epidermis appeared to be normal at that time point (Fig. 4A).

Inactivating *Fntb* in mouse embryonic fibroblasts abolishes their ability to proliferate (M. Liu *et al*., submitted for publication). To determine whether *Fntb* deficiency in keratinocytes causes a similar proliferation abnormality, equal numbers of keratinocytes from P1 $Fntb^{\Delta/\Delta}$ and $Fntb^{+/\Delta}$ mice were seeded into culture dishes. $Fntb^{+/\Delta}$ keratinocytes proliferated in a robust fashion, whereas $Fntb^{\Delta/\Delta}$ keratinocyte cultures were sparse and the cells had a flattened morphology (Fig. 7A). Cell counting confirmed a marked proliferation defect in $Fntb^{\Delta/\Delta}$ keratinocytes (Fig. 7B and C).

The same experimental approach was used to assess the importance of GGTase-I in stratified epithelium. A conditional knockout allele for *Pggt1b, Pggt1b*^{fl} (41) and the *KCre* transgene was used to produce keratinocyte-specific *Pggt1b* knockout mice ($Pggt1b^{fl/fl}KCre^{+}$, designated $Pggt1b^{\Delta/\Delta}$). The Cre-mediated recombination event excised exon 7 from *Pggt1b*, eliminating the catalytic site of the enzyme and yielding a frameshift (41). $Pggt1b^{\Delta/\Delta}$ keratinocytes had negligible levels of *Pggt1b* transcripts, as judged by quantitative PCR ($0.8 \pm 0.2\%$ of those in wild-type mice; $n = 2$ wild-type and $n = 4$ $Pggt1b^{\Delta/\Delta}$ keratinocyte preparations). The β-subunit of GGTase-I was undetectable in keratinocytes by western blotting (Fig. 8A). As expected, non-prenylated RAP1 (a protein that is normally geranylgeranylated) accumulated in $Pggt1b^{\Delta/\Delta}$ keratinocytes (Fig. 8B).

$Pggt1b^{\Delta/\Delta}$ mice survived development and were born at the expected Mendelian ratios, but died within a few hours of birth. At the time that the mice died, they invariably had little milk in their stomach. Histological studies of E19.5 $Pggt1b^{\Delta/\Delta}$ embryos revealed stunted hair follicles, but the interfollicular epidermis appeared normal (Fig. 8C). The skin barrier was intact in $Pggt1b^{\Delta/\Delta}$ mice (Supplementary Material, Fig. S3B). Even though no abnormalities were identified in the interfollicular epidermis of $Pggt1b^{\Delta/\Delta}$ mice, $Pggt1b^{\Delta/\Delta}$ epidermal keratinocytes did not proliferate in culture (Fig. 8D).

$Fntb^{fl/fl}Pggt1b^{fl/fl}$ and $Fntb^{fl/+}Pggt1b^{fl/+}KCre^{+}$ mice were intercrossed with the goal of generating $Fntb^{\Delta/\Delta}Pggt1b^{\Delta/\Delta}$ embryos. A few $Fntb^{\Delta/\Delta}Pggt1b^{\Delta/\Delta}$ embryos were identified. At E17.5, $Fntb^{\Delta/\Delta}Pggt1b^{\Delta/\Delta}$ embryos had fewer hair follicles,

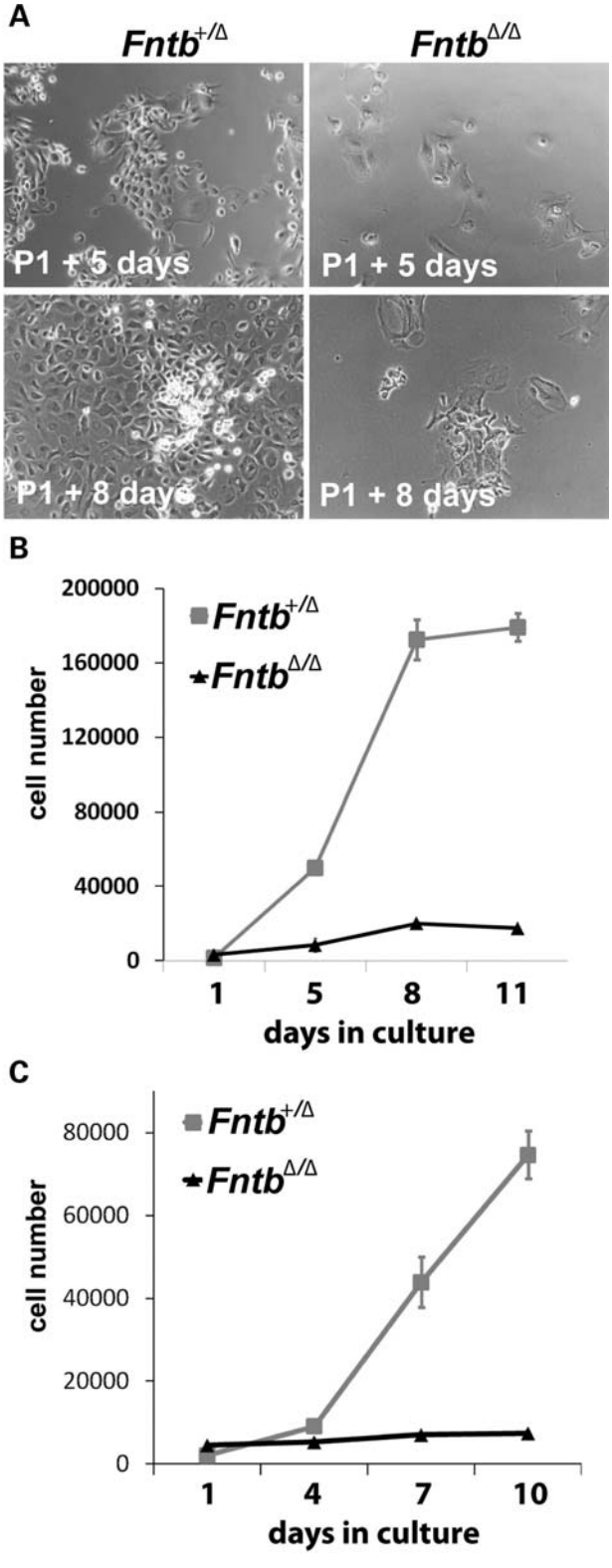

Figure 7. *Fntb* deficiency abolishes the ability of keratinocytes to proliferate. (**A**) Phase contrast images of keratinocytes from P1 $Fntb^{+/\Delta}$ and $Fntb^{\Delta/\Delta}$ mice after 5 or 8 days in culture. (**B, C**) Quantitative analysis of keratinocyte growth. Equal numbers of keratinocytes from $Fntb^{+/\Delta}$ and $Fntb^{\Delta/\Delta}$ mice at P1 (B) and P4 (C) were plated on 24-well plates. At the indicated time points, cells (3 wells/genotype) were counted. Data are representative of three independent experiments.

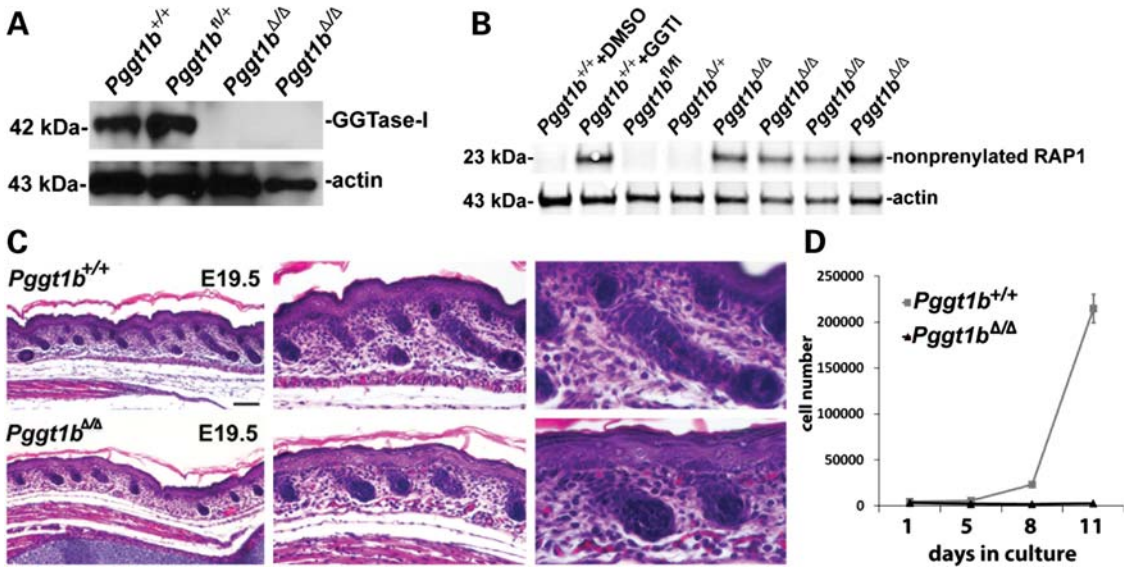

Figure 8. Inactivating GGTase-I in skin keratinocytes. (**A**) Western blot of keratinocytes from *Pggt1b*$^{+/+}$and *Pggt1b*$^{\Delta/\Delta}$ mice with an antibody against the β-subunit of GGTase-I. Actin was used as a loading control. (**B**) Western blot of keratinocyte extracts with an antibody that recognizes the non-prenylated form of RAP1. As a positive control, we used *Pggt1b*$^{+/+}$cells that had been treated with an inhibitor of GGTase-I (GGTI-298, 10 μM). (**C**) Hematoxylin and eosin-stained sections of skin from wild-type and *Pggt1b*$^{\Delta/\Delta}$ keratinocytes at E19.5, revealing stunted hair follicle growth in *Pggt1b*$^{\Delta/\Delta}$ mice. The interfollicular epidermis appeared normal (same image is shown at 10×, 20× and 40×). (**D**) Quantitative analysis of keratinocyte growth in culture. Equal numbers of keratinocytes from *Pggt1b*$^{+/+}$ and *Pggt1b*$^{\Delta/\Delta}$ mice at E19.5 were plated on 24-well dishes, and cell proliferation was monitored for 10 days.

and the interfollicular epidermis was slightly thinner compared with skin from mice lacking only *Fntb* or only *Pggt1b* (Fig. 9A and B). Immunohistochemical studies of E17.5 *Fntb*$^{\Delta/\Delta}$*Pggt1b*$^{\Delta/\Delta}$ skin revealed more apoptotic cells than in embryos lacking only *Fntb* or only *Pggt1b* (Fig. 9C).

DISCUSSION

We used conditional knockout alleles for *Fntb* and *Pggt1b* and a keratin 14–Cre transgene to produce mice lacking FTase or GGTase-I in skin keratinocytes (*Fntb*$^{\Delta/\Delta}$ and *Pggt1b*$^{\Delta/\Delta}$ mice). Skin keratinocytes from *Fntb*$^{\Delta/\Delta}$ mice had negligible levels of *Fntb* transcripts, and the β-chain of FTase was undetectable by western blotting. Similarly, only trace amounts of *Pggt1b* transcripts could be detected in *Pggt1b*$^{\Delta/\Delta}$ keratinocytes, and the β-chain of GGTase-I was undetectable by western blotting. Both *Fntb*$^{\Delta/\Delta}$ and *Pggt1b*$^{\Delta/\Delta}$ mice exhibited clear phenotypes. The hair follicles of *Fntb*$^{\Delta/\Delta}$ mice were small and dysmorphic, and the mice developed severe alopecia. Immunohistochemical and ultrastructural studies revealed apoptotic cells in hair follicles, providing a likely explanation for alopecia. Hair follicles in *Pggt1b*$^{\Delta/\Delta}$ mice were stunted, and the mice invariably died soon after birth. The reason for their perinatal demise is uncertain. The keratin 14–Cre transgene is known to induce recombination in the oropharynx, esophagus and stomach (45), and we initially thought that we might uncover significant pathology in those tissues. However, no pathology was detected. Interestingly, stunted hair growth and unexplained death were also observed when a keratin 14–Cre transgene was used to inactivate *Rac1* (a geranylgeranylated GTPase) in keratinocytes (46); those investigators suspected that they might identify pathology in the oropharynx or esophagus, but none was found. At this point, we simply do not understand why *Pggt1b* deficiency in keratinocytes yields a more lethal phenotype than *Fntb* deficiency.

Deficiencies of *Fntb* or *Pggt1b* lead to pathology in hair follicles, but minimal abnormalities in the interfollicular epidermis. Similar findings were observed in keratinocyte-specific *Rac1* knockout mice (46). The keratin 14 promoter driving Cre recombinase is equally active in the interfollicular epidermis and hair follicles, so the absence of visible effects in the interfollicular epidermis suggests that the protein substrates of FTase are either less essential in interfollicular epidermis or the apoptotic cells are replaced more efficiently in that location. The sparing of the interfollicular epidermis from significant pathology cannot be ascribed to inefficient gene inactivation. First, we isolated keratinocytes from sheets of skin epidermis, and western blot and qRT–PCR studies on those cells revealed that the knockouts were very efficient. Secondly, non-farnesylated DNAJA1 accumulated in skin keratinocytes from *Fntb*$^{\Delta/\Delta}$ mice and non-prenylated RAP1 accumulated in *Pggt1b*$^{\Delta/\Delta}$ keratinocytes. Thirdly, HRAS in *Fntb*$^{\Delta/\Delta}$ keratinocytes was found in the cytosolic (S100) fraction of cells rather than in the membrane (P100) fraction. Finally, keratinocytes from *Fntb*$^{\Delta/\Delta}$ and *Pggt1b*$^{\Delta/\Delta}$ mice were unable to proliferate in culture. The latter finding was consistent with the inability of *Fntb*- or *Pggt1b*-deficient fibroblasts to proliferate in culture (M. Liu *et al*., submitted for publication) (41).

The finding of profound alopecia in keratinocyte-specific *Fntb* knockout mice contrasts with earlier work on *Fntb* deficiency in mice. Mijimolle *et al*. (33) developed a conditional knockout allele for *Fntb* and used an inducible Cre transgene to inactivate FTase in many tissues. In their hands, FTase deficiency did not lead to pathology in the skin or any other tissue, leading them to conclude that FTase was

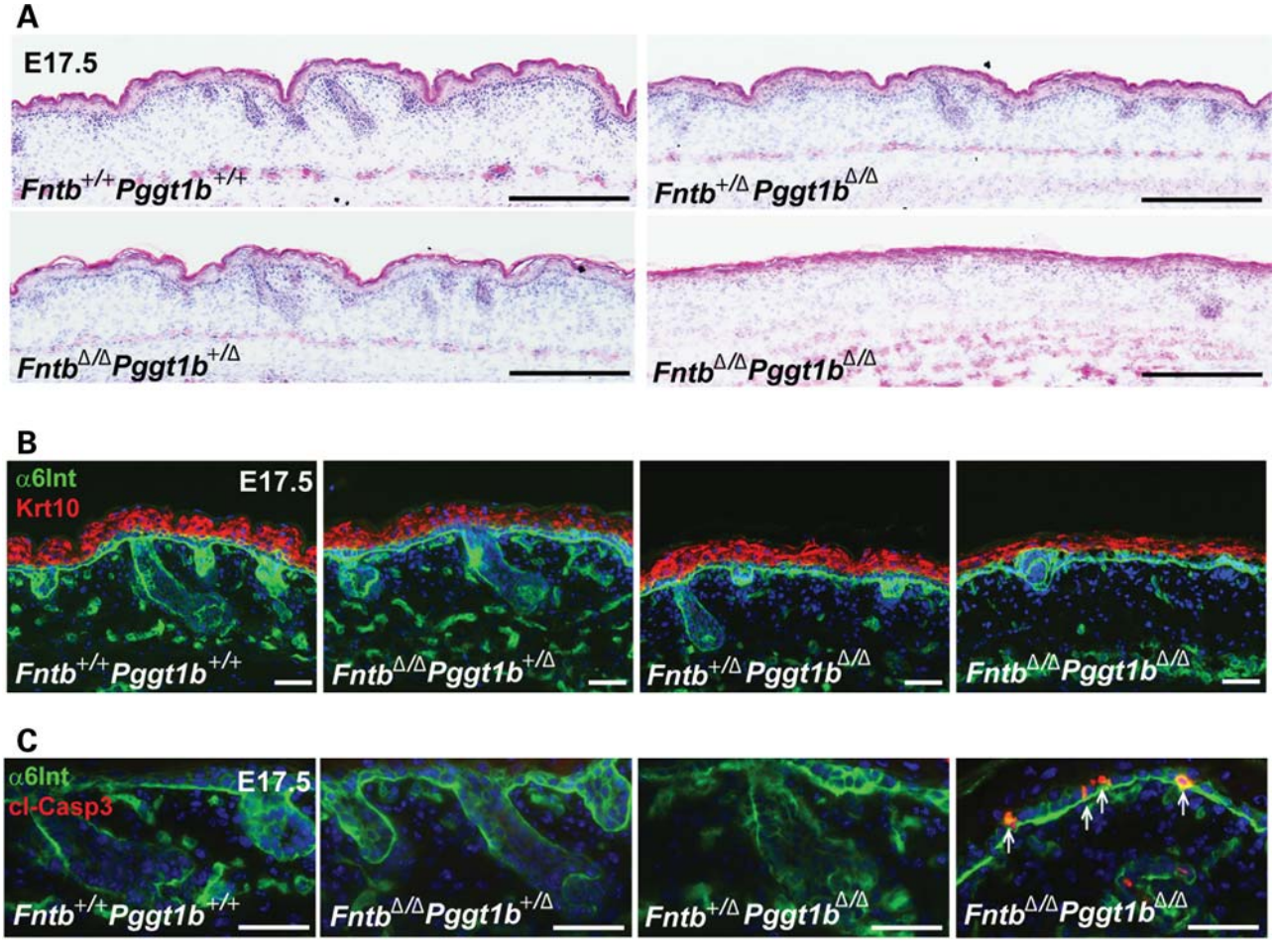

Figure 9. Inactivating both FTase and GGTase-I results in fewer hair follicles and a thinner interfollicular epidermis at E17.5. (**A**) Hematoxylin and eosin-stained sections of skin from *Fntb*$^{+/+}$*Pggt1b*$^{+/+}$, *Fntb*$^{+/\Delta}$*Pggt1b*$^{\Delta/\Delta}$, *Fntb*$^{\Delta/\Delta}$*Pggt1b*$^{+/\Delta}$ and *Fntb*$^{\Delta/\Delta}$*Pggt1b*$^{\Delta/\Delta}$ embryos at E17.5. Hair follicle development in *Fntb*$^{\Delta/\Delta}$ *Pggt1b*$^{\Delta/\Delta}$ embryos was stunted, and the skin was thinner, compared with mice lacking only FTase or only GGTase-I. (**B**) Staining for the spinous layer of the epidermis with an antibody against keratin 10 (Krt10, red) highlighted the thinning of the interfollicular epidermis in *Fntb*$^{\Delta/\Delta}$*Pggt1b*$^{\Delta/\Delta}$ embryos. (**C**) Immunohistochemical studies with an antibody against the cleaved form of caspase 3 (cl-Casp3, red), revealing apoptotic epidermal cells in E17.5 *Fntb*$^{\Delta/\Delta}$*Pggt1b*$^{\Delta/\Delta}$ epidermis (arrows). Scale bars indicate 50 μm for (B and C) and 500 μm for (A).

dispensable. However, they found that *Fntb* deficiency yielded only a partial blockade of DNAJA1 prenylation and did not block the ability of HRAS to associate with membranes. In our *Fntb*$^{\Delta/\Delta}$ mice, we found severe alopecia, a near-complete inhibition of DNAJA1 prenylation in keratinocytes, and a striking inability of HRAS to associate with membranes. Also, Mijimolle *et al*. (33) found that FTase-deficient fibroblasts grew in culture, but in our hands, FTase deficiency eliminated the growth of both fibroblasts and keratinocytes. We do not understand all of the discrepancies between our results and the other study (33), but it is possible, perhaps even likely, that Mijimolle's knockout was incomplete. Yang *et al*. (40) analysed Mijimolle's *Fntb* knockout allele in more detail and showed that their 'knockout allele' yielded a previously unrecognized transcript specifying an in-frame deletion, and it is therefore possible that the transcript yielded an enzyme with residual function. Another possible explanation for Mijimolle's findings was that the level of recombination from their inducible *Cre* transgene was simply low. In any case, our results show that FTase is not dispensable in mouse tissues.

Our studies revealed that *Fntb* deficiency interferes with the conversion of prelamin A to mature lamin A, resulting in a striking accumulation of non-farnesylated prelamin A on western blots. Also, by taking advantage of a new rat monoclonal antibody against prelamin A (7G11), we showed an accumulation of prelamin A in the skin keratinocytes of *Fntb*$^{\Delta/\Delta}$ mice by immunohistochemistry. We did not observe any accumulation of prelamin A in the dermal fibroblasts of *Fntb*$^{\Delta/\Delta}$ mice, nor did we uncover any accumulation of prelamin A in wild-type mice or *Pggt1b*$^{\Delta/\Delta}$ mice. It was interesting that most of the prelamin A in *Fntb*$^{\Delta/\Delta}$ keratinocytes was located at the nuclear rim adjacent to the nuclear membrane rather than in the nucleoplasm. The laboratory of Dr Michael Sinensky had reported that the non-prenylated prelamin A in lovastatin- or FTI-treated fibroblasts is located in the nucleoplasm (47,48), suggesting that prenylation is required for targeting of prelamin A to the nuclear rim. In the current studies, we show that, *in vivo*, an absence of farnesylation does not prevent prelamin A from reaching the nuclear rim, presumably because other targeting mechanisms are operative. We have recently verified, with an independent

genetic approach, that non-farnesylated prelamin A is capable of reaching the nuclear rim. We generated knockin mice expressing non-prenylated prelamin A (by eliminating the cysteine of prelamin A's *CaaX* motif) and showed by immunohistochemistry that the prelamin A in those mice is targeted to the nuclear rim (B.S.J.D., S.G.Y. and L.G.F., unpublished data).

The biogenesis of mature lamin A from its precursor, prelamin A, involves a series of four post-translational processing steps, beginning with protein farnesylation (18,49,50). For many years, dogma held that prelamin A is farnesylated and that none of the subsequent processing steps occurs in the absence of protein farnesylation (18,49,50). However, recent studies by Varela *et al*. (51) have contested this view, arguing that prelamin A might be prenylated efficiently by GGTase-I when FTase is inhibited. They went on to argue that combined FTase and GGTase-I inhibition would be important for the treatment of progeria (a disease caused by the accumulation of a farnesylated form of prelamin A). If prelamin A were truly processed efficiently by GGTase-I in the absence of FTase, one would predict that FTase deficiency would result in the minimal accumulation of prelamin A and fairly normal levels of lamin A biogenesis. Our results would provide little support for these predictions. FTase deficiency in keratinocytes led to a striking accumulation of non-prenylated prelamin A, and western blots of keratinocyte extracts revealed that the amount of prelamin A in cells exceeded that of mature lamin A. Our experiments cannot completely exclude the possibility that some fraction of prelamin A is geranylgeranylated, allowing for small amounts of lamin A biogenesis. However, our studies establish the primacy of FTase in prelamin A processing and argue against the idea that prelamin A processing and lamin A biogenesis proceed efficiently in the absence of FTase.

In summary, we show that both the *CaaX* protein prenyltransferases, FTase and GGTase-I, are important for the homeostasis of skin keratinocytes. FTase deficiency in keratinocytes leads to severe alopecia and is associated with apoptosis of keratinocytes. The latter findings dispel the notion that FTase is dispensable in adult tissues and argue that farnesylation is crucial in mammals, as it is in yeasts and plants (34,35). The finding that FTase is not dispensable in adult mammalian tissues should be of interest to those using FTIs to treat progeria and other human diseases. If FTase were entirely dispensable, as was suggested earlier (33), one might have reasonably expected that FTase inhibition would be safe. However, in view of the current genetic studies, clinicians testing FTIs in humans (27) should be attuned to the possibility that inhibiting FTase could lead to adverse side effects in normal tissues.

MATERIALS AND METHODS

Genetically modified mice

Mice harboring a new conditional knockout allele for *Fntb* (*Fntb*^{fl}) were recently created by Liu *et al*. (submitted for publication) and used to assess the impact of FTase deficiency on the growth of K-RAS^{G12D}-induced tumors. The *Fntb* conditional knockout allele contains one *loxP* site 1.0 kb upstream of exon 1 and another *loxP* site 1.0 kb downstream of the exon 1–intron 1 junction. Cre-mediated excision of the 'floxed' segment of *Fntb* removes the proximal promoter and the translation start site in exon 1. *Fntb*$^{+}$ and *Fntb*^{fl} alleles were identified by PCR of genomic DNA with forward primer 5′-AGGATTTGGGTGAGGGAA-3′ and reverse primer 5′-AGCAGCCACCTGGAGACT-3′. *Fntb*$^{+}$ and *Fntb*^{fl} alleles yield 250 and 320 bp DNA fragments, respectively. Mice harboring a conditional knockout allele for *Pggt1b* (*Pggt1b*^{fl}) were genotyped as described (41). Mice expressing a keratin 14–Cre (*KCre*) transgene (52) were obtained from The Jackson Laboratory. The presence of the *KCre* transgene was detected by PCR with forward primer 5′-GCATTACC GGTCGATGCAACGAGTGATGAG-3′ and reverse primer 5′-GAGTGAACGAACCTGGTCGAAATCAGTGCG-3′. All mouse experiments were approved by UCLA's Animal Research Committee.

Isolation and culture of mouse epidermal keratinocytes

Mouse epidermal keratinocytes were isolated from mouse skin on post-natal day 1 or 4 (P1 or P4) (53). Keratinocytes were counted with a Coulter counter, and equal numbers of cells were seeded into each well of a six-well tissue culture plate (Becton-Dickinson) along with mitotically inactivated 3T3 fibroblasts. Keratinocytes were cultured in Williams E medium with 0.15 mM Ca^{2+} in 5% CO_2 at 37°C (53). Each experiment with cultured keratinocytes was performed at least three times with keratinocytes prepared on different days. Images of keratinocytes were recorded on a Zeiss Axiovert 200 MOT inverted microscope with an Axiocam MR camera.

Epidermal barrier assay

The integrity of the mouse epidermis was assessed by established methods (54). Briefly, mouse pups at different stages of development (from E15.5 to E19.5) were collected, washed in phosphate-buffered saline (PBS) and placed in a phosphate buffer containing 2.45 mM X-gal (bromo-chloro-indolyl-galactopyranoside), pH 4.5. The pups were incubated in the X-gal solution with gentle agitation for 3–4 h at 37°C and then overnight at 4°C. In the absence of a functional barrier, X-gal enters the skin and is cleaved by endogenous β-galactosidase activity, resulting in blue skin.

Extraction of RNA, cDNA synthesis and RT–PCR

RNA isolation and cDNA synthesis were performed as described (55). Levels of *Fntb* and *Pggt1b* transcripts were determined by quantitative RT–PCR. For *Fntb*, we used oligonucleotides 5′-GACGGCTGCTACTCCTTCTG-3′ and 5′-TGCTGATGGAACATCCAATG-3′; for *Pggt1b*, we used oligonucleotides 5′-GGGCATGGATATGAAGAAAGC-3′ and 5′-AAGGTGGATCCTCCATGAGAC-3′.

Western blotting

Total cell extracts or subcellular fractions (4) from keratinocytes or tissues were size-fractionated on NuPAGE 4–12%

Bis–Tris gels (Invitrogen). For DNAJA1 western blots, samples were fractionated on 15% acrylamide/0.08% bisacrylamide sodium dodecyl sulfate gels. We used antibodies for the following proteins: H-RAS (sc-520, Santa Cruz Biotechnology, 1:200), non-prenylated RAP1A (sc-1482, 1:200), lamin A (sc-6215, 1:400), actin (sc-1616, 1:1000), FTaseβ (sc-137, 1:200), DNAJA1 (MS-225-P1, NeoMarkers, 1:400), GGTase-Iβ (Abnova, 1:500) and a rabbit polyclonal antibody against mouse prelamin A (43). Protein bands were visualized with IR-Dye 800CW- and IR-Dye 700DX-conjugated anti-goat, anti-mouse and anti-rabbit polyclonal antibodies (Rockland). Antibody binding was visualized with the Odyssey Infrared Imaging System (Li-Cor Biosciences). HRAS western blots were performed with a horseradish peroxidase-conjugated secondary antibody and the ECL Western Blotting System (both from GE Healthcare).

Histology and immunohistochemistry

For histological analysis, mouse tissues were fixed in 4% paraformaldehyde (PFA), embedded in paraffin, sectioned and stained with hematoxylin and eosin. For immunohistochemistry studies, mouse tissues were placed into optimum cutting temperature compound (Sakura), frozen on dry ice and sectioned with a cryostat (Microm or Leica). Slides were fixed in 4% formalin for 10 min, washed with PBS containing 0.1% Triton X-100 (PBS-T), incubated in blocking buffer (PBS containing 10% donkey or goat serum, 0.2% bovine serum albumin, 1 mM $CaCl_2$ and 1 mM $MgCl_2$) for 1 h, washed twice with PBS-T, incubated overnight with primary antibody diluted in blocking buffer containing 0.1% Triton X-100 and washed twice with PBS-T. Secondary antibodies were incubated in a similar manner for 0.5–1 h, and the slides were again washed with PBS-T. The slides were fixed with 4% PFA for 5 min and mounted with Vectashield with DAPI (Invitrogen). The following antibodies were used for the immunohistochemical studies: Keratin 14 (rabbit, 1:800, Covance), Integrin α6 (rat, 1:750, BD Pharmingen), Keratin 31 (guinea pig, 1:200, Covance), Keratin 10 (rabbit, 1:200, Covance), Loricrin (rabbit, 1:800, Covance), Sox9 (rabbit, 1:500, Chemicon), CDP (rabbit, 1:100, Santa Cruz Biotechnology), Ki67 (rabbit, 1:300, Novacastra), Phospho-Histone H3 (rat, 1:1100, Sigma) and Cleaved Caspase 3 (rabbit, 1:200, Cell Signaling Technology). Images were obtained on a Zeiss microscope with an Axiocam MR camera or an Olympus light microscope with a digital camera (Olympus). Image processing and analysis were performed with Photoshop CS4 (Adobe).

Development of a rat monoclonal against mouse prelamin A

Rats were immunized with a mouse prelamin A peptide corresponding to the C-terminal 18 amino acids of mouse prelamin A. Splenocytes were fused with myeloma cells, and stable hybridomas were selected. A rat monoclonal antibody against prelamin A, clone 7G11, was chosen for further analysis. Culture supernatants were prepared from high-density cultures and used for western blots and immunohistochemistry. For western blots, monoclonal antibody binding was detected with an IR-Dye 800-conjugated donkey anti-rat IgG (Li-Cor, 1:2000). For immunofluorescence studies, tissues frozen in OCT were sectioned and fixed in cold methanol for 10 min. Staining for lamin A/C (goat, 1:500, Santa Cruz Biotechnology) and prelamin A (7G11, 1:50) was performed as described earlier.

Electron microscopy

Cells were fixed in 2% glutaraldehyde, 2% PFA in 0.1 M sodium cacodylate buffer and washed. After incubating for 1 h in PBS containing 1% osmium tetroxide, the cells were dehydrated in a graded series of ethanol, treated with propylene oxide and embedded in Eponate 12 (Ted Pella). Thick sections (60–70 nm) were cut on a Reichert-Jung Ultracut E ultramicrotome and picked up on formvar-coated copper grids. The sections were stained with uranyl acetate and Reynolds lead citrate and examined on a JEOL 100CX electron microscope at 80 kV.

SUPPLEMENTARY MATERIAL

Supplementary Material is available at *HMG* online.

ACKNOWLEDGEMENT

We thank Marianne Cilluffo and Hilda Amalia Passoli for assistance with electron microscopy.

Conflict of Interest statement. None declared.

FUNDING

This work was supported by the National Institutes of Health grants (AR050200, HL76839, HL86683 and GM66152); March of Dimes Grant (6-FY2007-1012); the Ellison Medical Foundation Senior Scholar Program; a BSCRC CIRM training grant (T1-00005); the Maria Rowena Chair in Cell Biology; the Jonsson Cancer Center Foundation; the Cancer Research Coordinating Committee; the European Research Council; the Swedish Medical Research Council; the Swedish Cancer Society and Västra Götalandsregionen.

REFERENCES

1. Casey, P.J. and Seabra, M.C. (1996) Protein prenyltransferases. *J. Biol. Chem.*, **271**, 5289–5292.
2. Zhang, F.L. and Casey, P.J. (1996) Protein prenylation: molecular mechanisms and functional consequences. *Annu. Rev. Biochem.*, **65**, 241–269.
3. Boyartchuk, V.L., Ashby, M.N. and Rine, J. (1997) Modulation of Ras and a-factor function by carboxyl-terminal proteolysis. *Science*, **275**, 1796–1800.
4. Kim, E., Ambroziak, P., Otto, J.C., Taylor, B., Ashby, M., Shannon, K., Casey, P.J. and Young, S.G. (1999) Disruption of the mouse *Rce1* gene results in defective Ras processing and mislocalization of Ras within cells. *J. Biol. Chem.*, **274**, 8383–8390.
5. Otto, J.C., Kim, E., Young, S.G. and Casey, P.J. (1999) Cloning and characterization of a mammalian prenyl protein-specific protease. *J. Biol. Chem.*, **274**, 8379–8382.
6. Hrycyna, C.A., Sapperstein, S.K., Clarke, S. and Michaelis, S. (1991) The *Saccharomyces cerevisiae STE14* gene encodes a methyltransferase that

mediates C-terminal methylation of a-factor and Ras proteins. *EMBO J.*, **10**, 1699–1709.
7. Dai, Q., Choy, E., Chiu, V., Romano, J., Slivka, S.R., Steitz, S.A., Michaelis, S. and Philips, M.R. (1998) Mammalian prenylcysteine carboxyl methyltransferase is in the endoplasmic reticulum. *J. Biol. Chem.*, **273**, 15030–15034.
8. Silvius, J.R. and l'Heureux, F. (1994) Fluorimetric evaluation of the affinities of isoprenylated peptides for lipid bilayers. *Biochemistry*, **33**, 3014–3022.
9. Hancock, J.F., Magee, A.I., Childs, J.E. and Marshall, C.J. (1989) All *ras* proteins are polyisoprenylated but only some are palmitoylated. *Cell*, **57**, 1167–1177.
10. Casey, P.J., Solski, P.A., Der, C.J. and Buss, J.E. (1989) p21ras is modified by a farnesyl isoprenoid. *Proc. Natl Acad. Sci. USA*, **86**, 8323–8327.
11. Cox, A.D., Hisaka, M.M., Buss, J.E. and Der, C.J. (1992) Specific isoprenoid modification is required for function of normal, but not oncogenic, Ras protein. *Mol. Cell. Biol.*, **12**, 2606–2615.
12. James, G.L., Goldstein, J.L., Brown, M.S., Rawson, T.E., Somers, T.C., McDowell, R.S., Crowley, C.W., Lucas, B.K., Levinson, A.D. and Marsters, J.C. Jr (1993) Benzodiazepine peptidomimetics: potent inhibitors of Ras farnesylation in animal cells. *Science*, **260**, 1937–1942.
13. Tamanoi, F. (1993) Inhibitors of Ras farnesyltransferases. *Trends Biochem. Sci.*, **18**, 349–353.
14. Gibbs, J.B., Oliff, A. and Kohl, N.E. (1994) Farnesyltransferase inhibitors: Ras research yields a potential cancer therapeutic. *Cell*, **77**, 175–178.
15. Lerner, E.C., Hamilton, A.D. and Sebti, S.M. (1997) Inhibition of Ras prenylation: a signaling target for novel anti-cancer drug design. *Anticancer Drug Des.*, **12**, 229–238.
16. Kohl, N.E., Wilson, F.R., Mosser, S.D., Giuliani, E., DeSolms, S.J., Conner, M.W., Anthony, N.J., Holtz, W.J., Gomez, R.P., Lee, T.-J. *et al.* (1994) Protein farnesyltransferase inhibitors block the growth of *ras*-dependent tumors in nude mice. *Proc. Natl Acad. Sci. USA*, **91**, 9141–9145.
17. Lancet, J.E., Rosenblatt, J.D. and Karp, J.E. (2002) Farnesyltransferase inhibitors and myeloid malignancies: phase I evidence of Zarnestra activity in high-risk leukemias. *Semin. Hematol.*, **39**, 31–35.
18. Young, S.G., Fong, L.G. and Michaelis, S. (2005) Prelamin A, Zmpste24, misshapen cell nuclei, and progeria—new evidence suggesting that protein farnesylation could be important for disease pathogenesis. *J. Lipid Res.*, **46**, 2531–2558.
19. Worman, H.J., Fong, L.G., Muchir, A. and Young, S.G. (2009) Laminopathies and the long strange trip from basic cell biology to therapy. *J. Clin. Invest.*, **119**, 1825–1836.
20. Davies, B.S., Fong, L.G., Yang, S.H., Coffinier, C. and Young, S.G. (2009) The posttranslational processing of prelamin A and disease. *Annu. Rev. Genomics Hum. Genet.*, **10**, 153–174.
21. Toth, J.I., Yang, S.H., Qiao, X., Beigneux, A.P., Gelb, M.H., Moulson, C.L., Miner, J.H., Young, S.G. and Fong, L.G. (2005) Blocking protein farnesyltransferase improves nuclear shape in fibroblasts from humans with progeroid syndromes. *Proc. Natl Acad. Sci. USA*, **102**, 12873–12878.
22. Yang, S.H., Bergo, M.O., Toth, J.I., Qiao, X., Hu, Y., Sandoval, S., Meta, M., Bendale, P., Gelb, M.H., Young, S.G. *et al.* (2005) Blocking protein farnesyltransferase improves nuclear blebbing in mouse fibroblasts with a targeted Hutchinson–Gilford progeria syndrome mutation. *Proc. Natl Acad. Sci. USA*, **102**, 10291–10296.
23. Fong, L., Frost, D., Meta, M., Qiao, X., Yang, S., Coffinier, C. and Young, S. (2006) A protein farnesyltransferase inhibitor ameliorates disease in a mouse model of progeria. *Science*, **311**, 1621–1623.
24. Yang, S.H., Meta, M., Qiao, X., Frost, D., Bauch, J., Coffinier, C., Majumdar, S., Bergo, M.O., Young, S.G. and Fong, L.G. (2006) Treatment with a protein farnesyltransferase inhibitor improves disease phenotypes in mice with a targeted Hutchinson–Gilford progeria syndrome mutation. *J. Clin. Invest.*, **116**, 2115–2121.
25. Yang, S.H., Qiao, X., Fong, L.G. and Young, S.G. (2008) Treatment with a farnesyltransferase inhibitor improves survival in mice with a Hutchinson–Gilford progeria syndrome mutation. *Biochim. Biophys. Acta*, **1781**, 36–39.
26. Yang, S.H., Chang, S.Y., Andres, D.A., Spielmann, H.P., Young, S.G. and Fong, L.G. (2010) Assessing the efficacy of protein farnesyltransferase inhibitors in mouse models of progeria. *J. Lipid Res.*, **51**, 400–405.
27. Kieran, M.W., Gordon, L. and Kleinman, M. (2007) New approaches to progeria. *Pediatrics*, **120**, 834–841.
28. Cox, A.D. and Der, C.J. (1997) Farnesyltransferase inhibitors and cancer treatment: targeting simply Ras? *Biochim. Biophys. Acta*, **1333**, F51–F71.
29. Gibbs, J.B., Graham, S.L., Hartman, G.D., Koblan, K.S., Kohl, N.E., Omer, C.A. and Oliff, A. (1997) Farnesyltransferase inhibitors versus Ras inhibitors. *Curr. Opin. Chem. Biol.*, **1**, 197–203.
30. Gibbs, J.B. and Oliff, A. (1997) The potential of farnesyltransferase inhibitors as cancer chemotherapeutics. *Annu. Rev. Pharmacol. Toxicol.*, **37**, 143–166.
31. Maurer-Stroh, S., Koranda, M., Benetka, W., Schneider, G., Sirota, F.L. and Eisenhaber, F. (2007) Towards complete sets of farnesylated and geranylgeranylated proteins. *PLoS Comput. Biol.*, **3**, e66.
32. Reid, T.S., Terry, K.L., Casey, P.J. and Beese, L.S. (2004) Crystallographic analysis of CaaX prenyltransferases complexed with substrates defines rules of protein substrate selectivity. *J. Mol. Biol.*, **343**, 417–433.
33. Mijimolle, N., Velasco, J., Dubus, P., Guerra, C., Weinbaum, C.A., Casey, P.J., Campuzano, V. and Barbacid, M. (2005) Protein farnesyltransferase in embryogenesis, adult homeostasis, and tumor development. *Cancer Cell*, **7**, 313–324.
34. Powers, S., Michaelis, S., Broek, D., Anna-A, S.S., Field, J., Herskowitz, I. and Wigler, M. (1986) *RAM*, a gene of yeast required for a functional modification of *RAS* proteins and for production of mating pheromone **a**-factor. *Cell*, **47**, 413–422.
35. Yalovsky, S., Kulukian, A., Rodriguez-Concepcion, M., Young, C.A. and Gruissem, W. (2000) Functional requirement of plant farnesyltransferase during development in *Arabidopsis*. *Plant Cell*, **12**, 1267–1278.
36. Berzat, A.C., Brady, D.C., Fiordalisi, J.J. and Cox, A.D. (2006) Using inhibitors of prenylation to block localization and transforming activity. *Methods Enzymol.*, **407**, 575–597.
37. Berzat, A.C., Buss, J.E., Chenette, E.J., Weinbaum, C.A., Shutes, A., Der, C.J., Minden, A. and Cox, A.D. (2005) Transforming activity of the Rho family GTPase, Wrch-1, a Wnt-regulated Cdc42 homolog, is dependent on a novel carboxyl-terminal palmitoylation motif. *J. Biol. Chem.*, **280**, 33055–33065.
38. Chenette, E.J., Abo, A. and Der, C.J. (2005) Critical and distinct roles of amino- and carboxyl-terminal sequences in regulation of the biological activity of the Chp atypical Rho GTPase. *J. Biol. Chem.*, **280**, 13784–13792.
39. Takahashi, K., Nakagawa, M., Young, S.G. and Yamanaka, S. (2005) Differential membrane localization of ERas and Rheb, two Ras-related proteins involved in the phosphatidylinositol 3-kinase/mTOR pathway. *J. Biol. Chem.*, **280**, 32768–32774.
40. Yang, S.H., Bergo, M.O., Farber, E., Qiao, X., Fong, L.G. and Young, S.G. (2009) Caution! Analyze transcripts from conditional knockout alleles. *Transgenic Res.*, **18**, 483–489.
41. Sjogren, A.K., Andersson, K.M., Liu, M., Cutts, B.A., Karlsson, C., Wahlstrom, A.M., Dalin, M., Weinbaum, C., Casey, P.J., Tarkowski, A. *et al.* (2007) GGTase-I deficiency reduces tumor formation and improves survival in mice with K-RAS-induced lung cancer. *J. Clin. Invest.*, **117**, 1294–1304.
42. Schneider, M.R., Schmidt-Ullrich, R. and Paus, R. (2009) The hair follicle as a dynamic miniorgan. *Curr. Biol.*, **19**, R132–R142.
43. Fong, L.G., Ng, J.K., Lammerding, J., Vickers, T.A., Meta, M., Cote, N., Gavino, B., Qiao, X., Chang, S.Y., Young, S.R. *et al.* (2006) Prelamin A and lamin A appear to be dispensable in the nuclear lamina. *J. Clin. Invest.*, **116**, 743–752.
44. Nowak, J.A., Polak, L., Pasolli, H.A. and Fuchs, E. (2008) Hair follicle stem cells are specified and function in early skin morphogenesis. *Cell Stem Cell*, **3**, 33–43.
45. Andl, T., Ahn, K., Kairo, A., Chu, E.Y., Wine-Lee, L., Reddy, S.T., Croft, N.J., Cebra-Thomas, J.A., Metzger, D., Chambon, P. *et al.* (2004) Epithelial Bmpr1a regulates differentiation and proliferation in postnatal hair follicles and is essential for tooth development. *Development*, **131**, 2257–2268.
46. Castilho, R.M., Squarize, C.H., Patel, V., Millar, S.E., Zheng, Y., Molinolo, A. and Gutkind, J.S. (2007) Requirement of Rac1 distinguishes follicular from interfollicular epithelial stem cells. *Oncogene*, **26**, 5078–5085.
47. Lutz, R.J., Trujillo, M.A., Denham, K.S., Wenger, L. and Sinensky, M. (1992) Nucleoplasmic localization of prelamin A: implications for prenylation-dependent lamin A assembly into the nuclear lamina. *Proc. Natl Acad. Sci. USA*, **89**, 3000–3004.

48. Dalton, M.B., Fantle, K.S., Bechtold, H.A., DeMaio, L., Evans, R.M., Krystosek, A. and Sinensky, M. (1995) The farnesyl protein transferase inhibitor BZA-5B blocks farnesylation of nuclear lamins and p21ras but does not affect their function or localization. *Cancer Res.*, **55**, 3295–3304.
49. Beck, L.A., Hosick, T.J. and Sinensky, M. (1990) Isoprenylation is required for the processing of the lamin A precursor. *J. Cell Biol.*, **110**, 1489–1499.
50. Sinensky, M., Fantle, K., Trujillo, M., McLain, T., Kupfer, A. and Dalton, M. (1994) The processing pathway of prelamin A. *J. Cell Sci.*, **107**, 61–67.
51. Varela, I., Pereira, S., Ugalde, A.P., Navarro, C.L., Suarez, M.F., Cau, P., Cadinanos, J., Osorio, F.G., Foray, N., Cobo, J. *et al.* (2008) Combined treatment with statins and aminobisphosphonates extends longevity in a mouse model of human premature aging. *Nat. Med.*, **14**, 767–772.
52. Dassule, H.R., Lewis, P., Bei, M., Maas, R. and McMahon, A.P. (2000) Sonic hedgehog regulates growth and morphogenesis of the tooth. *Development*, **127**, 4775–4785.
53. Blanpain, C., Lowry, W.E., Geoghegan, A., Polak, L. and Fuchs, E. (2004) Self-renewal, multipotency, and the existence of two cell populations within an epithelial stem cell niche. *Cell*, **118**, 635–648.
54. Hardman, M.J., Sisi, P., Banbury, D.N. and Byrne, C. (1998) Patterned acquisition of skin barrier function during development. *Development*, **125**, 1541–1552.
55. Beigneux, A.P., Davies, B., Gin, P., Weinstein, M.M., Farber, E., Qiao, X., Peale, P., Bunting, S., Walzem, R.L., Wong, J.S. *et al.* (2007) Glycosylphosphatidylinositol-anchored high density lipoprotein-binding protein 1 plays a critical role in the lipolytic processing of chylomicrons. *Cell Metab.*, **5**, 279–291.
56. Moulson, C.L., Go, G., Gardner, J.M., van der Wal, A.C., Smitt, J.H., van Hagen, J.M. and Miner, J.H. (2005) Homozygous and compound heterozygous mutations in ZMPSTE24 cause the laminopathy restrictive dermopathy. *J. Invest. Dermatol.*, **125**, 913–919.